# Antarctic Isotope Maxima events 24 and 25 identified in benthic marine $\delta^{18}$ O

Rocio P. Caballero-Gill, 1 Steve Clemens, 1 and Warren Prell1

Received 21 December 2011; revised 4 February 2012; accepted 7 February 2012; published 8 March 2012.

[1] High-resolution planktic and benthic  $\delta^{18}O$  records at Site 1146 (northern South China Sea) include structure within Marine Isotope Stage 5.4, 118.5–105.9 ka, that is not captured in stacked  $\delta^{18}O$  records commonly used for age model construction and as proxies for global ice volume. Leveraging a common monsoonal influence, Site 1146 planktic  $\delta^{18}O$  was aligned to speleothem  $\delta^{18}O$  from southeastern China to derive a radiometrically calibrated (RC) age model. On the RC age model, the benthic  $\delta^{18}O$  record contains structure equivalent in time to Antarctic Isotope Maximum (AIM) events 24 and 25. Sea level reconstructions for isotopic event 5.4 suggest that these benthic  $\delta^{18}O$  events (AIM 24 and 25) derive from isotopic change (ice volume) although some temperature change cannot be completely excluded.

Citation: Caballero-Gill, R. P., S. Clemens, and W. Prell (2012), Antarctic Isotope Maxima events 24 and 25 identified in benthic marine  $\delta^{18}$ O, *Paleoceanography*, 27, PA1101, doi:10.1029/2011PA002269.

## 1. Introduction

[2] Isotopic time series from the Greenland Ice Core Project (GRIP) and Greenland Ice Sheet Project (GISP) obtained during the early 1990s document abrupt, highfrequency climate change during the last glacial stage [Greenland Ice-Core Project Members, 1993; Grootes et al., 1993]. More recently, these high-frequency climate oscillations, known as Dansgaard-Oeschger (DO) events, have been identified in a variety of locations and archives that reflect changes in surface processes [Voelker, 2002]. A recent North GRIP (NGRIP) ice core identified DO events 24 and 25 (~105-114 ka), which have been linked to changes in North Atlantic surface δ18O [Greenland Ice-Core Project Members, 2004]. Similarly, 25 Antarctic warming events commonly referred to as Antarctic Isotope Maxima (AIM), have been identified in Antarctic ice core  $\delta^{18}$ O records [Capron et al., 2010].

[3] When compared using a CH<sub>4</sub>-synchronized timescale [Capron et al., 2010], the ice core  $\delta^{18}$ O variability from Greenland is out of phase relative to that in Antarctica (Figure 1). The bipolar seesaw concept is the leading candidate to explain this out of phase relationship observed in millennial-scale  $\delta^{18}$ O structure in the Greenland and Antarctica ice cores [Broecker, 1998; Stocker and Johnsen, 2003]. Given the global nature of these events, one might expect the events are linked to changing ice volume and thus should be expressed in the benthic  $\delta^{18}$ O record. To date, AIM structure in benthic marine  $\delta^{18}$ O during the last

interglacial has only been identified in the North Atlantic [Martrat et al., 2007].

[4] Our study documents these events in new high-resolution planktic and benthic foraminifera  $\delta^{18}O$  records generated from Ocean Drilling Program (ODP) 1146 in the South China Sea (SCS). The planktic  $\delta^{18}O$  at this site is synchronized to speleothem  $\delta^{18}O$ , yielding a radiometrically calibrated (RC) age model, which is transferred to the benthic  $\delta^{18}O$  from the same samples. Comparison of the benthic  $\delta^{18}O$  with speleothem  $\delta^{18}O$  indicates that the millennial-scale structure within Marine Isotope Stage (MIS) 5.4 match AIM 24 and 25, linking global-scale deep-ocean circulation and abrupt climate change.

# 2. Background

[5] Summer and winter monsoon circulation similarly influence cave speleothem sites in Southeast Asia and ODP Site 1146 in the northern SCS (Figure 2). During boreal summer, the northern hemisphere experiences high insolation, generating a low-pressure cell over Asia that is fed by inter-hemisphere transport of water vapor from the south. The study area experiences summer southerly winds at 3 to 6 m/s, and precipitation of 4 to 9 mm/day. Surface air temperatures range from ~24°C to 28°C at both sites. The winter season at these sites is characterized by cool, dry, northerly winds mainly influenced by the strong highpressure cell that develops over Mongolia. Wind speeds are on the order of 4 to 7 m/s and precipitation rates are less than 2 mm/day. Although the northern SCS and southeastern China experience synchronous seasonal cycles, a distinct seasonal gradient exists in surface air temperature, ~6°C at ODP 1146 and ~19°C at the cave sites [Kalnay et al., 1996]. At the glacial-interglacial time scales, both the northern SCS and southern China experience similar large-magnitude temperature and precipitation changes. The ensemble mean

Copyright 2012 by the American Geophysical Union. 0883-8305/12/2011PA002269

PA1101 1 of 7

<sup>&</sup>lt;sup>1</sup>Department of Geological Sciences, Brown University, Providence, Rhode Island, USA.

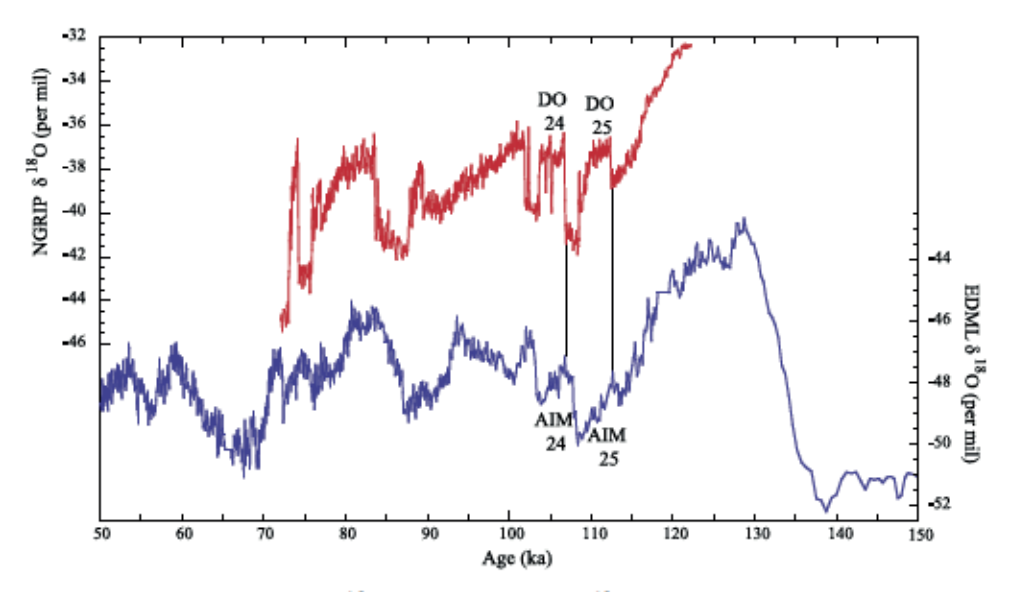


Figure 1. Bipolar seesaw. NGRIP  $\delta^{18}$ O (red) and EDML  $\delta^{18}$ O (blue) with corresponding DO events in Greenland out of phase with respect to AIM events in Antarctica (see text). Both ice cores are plotted using latest methane-synchronized age model [Ruth et al., 2007; Capron et al., 2010].

of seven Paleoclimate Modeling Intercomparison Project 2 (PMIP2) simulations indicate a 3.5°C cooling of annual surface temperatures during glacials at the speleothem and northern South China Sea sites [Jiang et al., 2011]. Evaporation at the sites decreased within the range of 20 to 25%, and precipitation within the range of 20 to 45% [Jiang et al., 2011]. At the precession time scale, insolation-only forcing

yields a 1 to 2°C and 0.14 to 0.37 mm/day precipitation range at both sites [Kutzbach et al., 2008].

[6] These similar environmental forcings and transports are recorded by the carbonate  $\delta^{18}$ O in cave speleothems and in surface ocean planktic foraminifera. The surface dwelling planktic foraminifera Globigerinoides ruber (Gs. ruber) reproduces year-round in the SCS [Tian et al., 2005], with

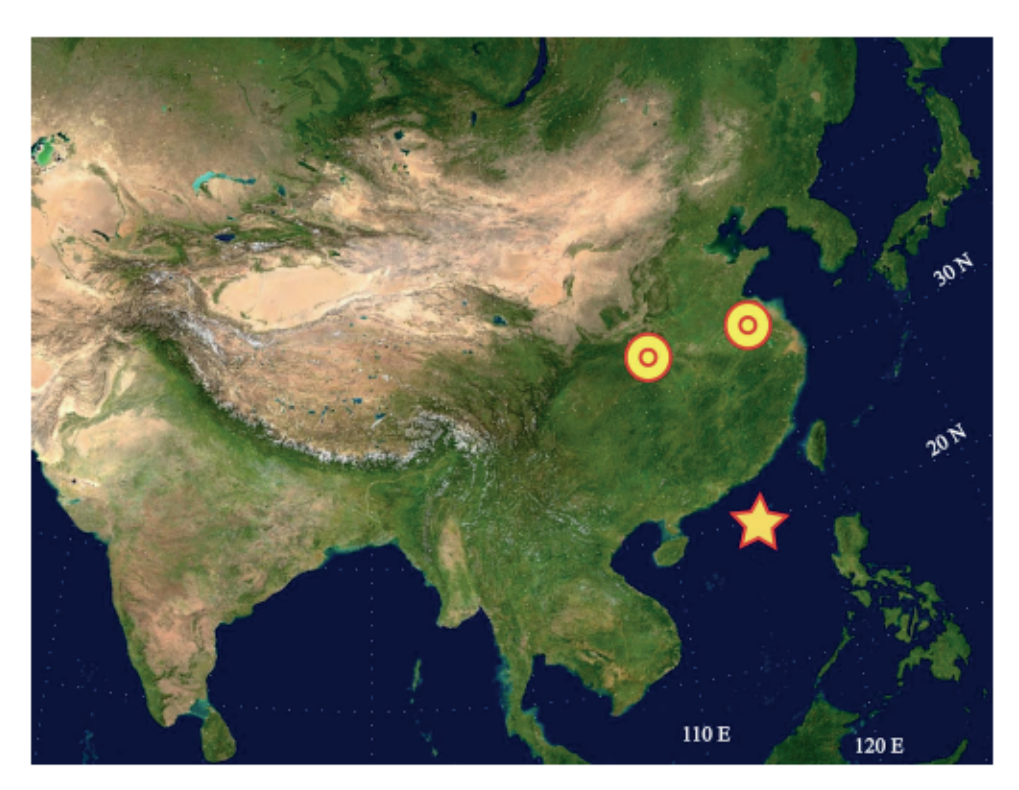


Figure 2. Satellite image of the study area. A star denotes the location of ODP 1146, and the two bull'seye symbols indicate the locations of caves Hulu (closer to the coast) and Sanbao (inland). Map is available at http://www.zonu.com.

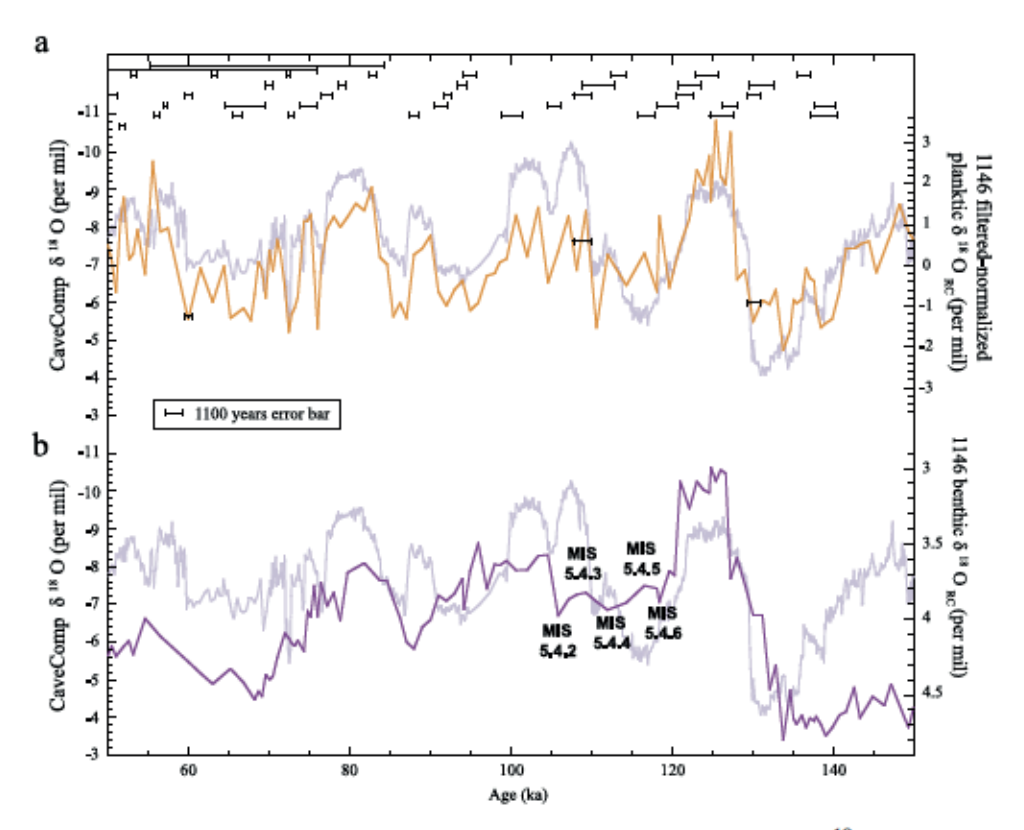


Figure 3. ODP 1146 RC age model: (a) alignment between ODP 1146 planktic  $\delta^{18}O$  (orange) and cave speleothem  $\delta^{18}O$  (light purple). Age errors associated with tie points used to create age model are plotted on the ODP 1146 planktic  $\delta^{18}O$ . Error bars at the top represent radiometric ages (with error bars) for the CaveComp record. (b) ODP 1146 benthic  $\delta^{18}O$  (dark purple) alignment to the cave speleothem  $\delta^{18}O$  (light purple) using the age model obtained from the planktic-cave alignment. MIS 5 isotopic events are labeled on the ODP 1146 benthic  $\delta^{18}O$  record.

higher flux during spring and winter [Tian et al., 2005; Wiesner et al., 1996]. Thus, Gs. ruber δ18O records seasonal fluctuations in temperature and monsoon runoff [Steinke et al., 20081 in addition to ice volume. Speleothem  $\delta^{18}$ O from southeastern China is influenced by three distinct wind regimes, each with a specific moisture source and isotopic composition [Clemens et al., 2010]. Analysis of modern precipitation shows that summer, fall/winter, and spring account for 48%, 34%, and 18% of annual precipitation, respectively. The seasonal moisture sources have isotopic compositions of -8.73 \, -6.55 \, and -3.09 \, SMOW [Clemens et al., 2010]. The weighted annual average of all seasons accurately predicts the  $\bar{\delta}^{18}$ O value of modem speleothem calcite (Dongge cave [Wang et al., 2005]). Therefore, speleothem  $\delta^{18}O$  also incorporates the seasonal variations in the temperature and rainfall isotopic composition. At orbital and glacial-interglacial scales, both speleothem and planktic  $\delta^{\bar{1}8}O$  incorporate whole-ocean changes in  $\delta^{18}$ O of seawater as well as regional-scale changes of temperature and precipitation.

## 3. Materials and Methods

## 3.1. ODP 1146

[7] ODP Site 1146 (19° 27' N, 116° 16' E, in 2092 m water depth) is located in the monsoon-influenced region of the SCS, about 400 km south of Hong Kong (Figure 2).

ODP 1146 was sampled every  $\sim$ 1 kyr (18 cm) and standard procedures were followed for foraminiferal isotopic analysis [Clemens et al., 2008]. We report 126 planktic and 123 benthic analyses. External reproducibility based on repeated analyses of Brown Yule Marble (BYM, 63–150  $\mu$ m) yielded  $\delta^{18}$ O values of  $-6.56 \pm 0.07$  % (1  $\sigma$ , n = 39). External reproducibility based on repeated analyses of Carrara Marble (63–150  $\mu$ m) yielded  $\delta^{18}$ O values of  $-1.88 \pm 0.07$  % (1  $\sigma$ , n = 33). External reproducibility around MIS 5.4 based on replicate analyses of planktic and benthic foraminifera samples are  $\pm 0.06$  % for  $\delta^{18}$ O (n = 4) and  $\pm 0.08$  % for  $\delta^{18}$ O (n = 18), respectively.

# 3.2. Composite Speleothem Record

[8] A composite speleothem  $\delta^{18}$ O record (Figures 2 and 3) was generated based on data from two caves in southeastern China: Sanbao (110° 26′ E, 31° 40′ N, 1900 m. elevation) and Hulu (119° 10′ E, 32° 30′ N, 100 m elevation) [Wang et al., 2001, 2008]. Because of the consistent offset in  $\delta^{18}$ O observed between speleothem  $\delta^{18}$ O at higher elevation Sanbao relative to lower elevation Hulu, isotopic values from Sanbao were adjusted by 1.6 ‰ to match Hulu, [Wang et al., 2008]. The composite record uses speleothems 11, 22, 23, and 25 from Sanbao and speleothem MSL from Hulu. The speleothem  $\delta^{18}$ O record has 627 data points (Figure 3) and 35 radiometric dates with a typical error in age (2 $\sigma$ ) of

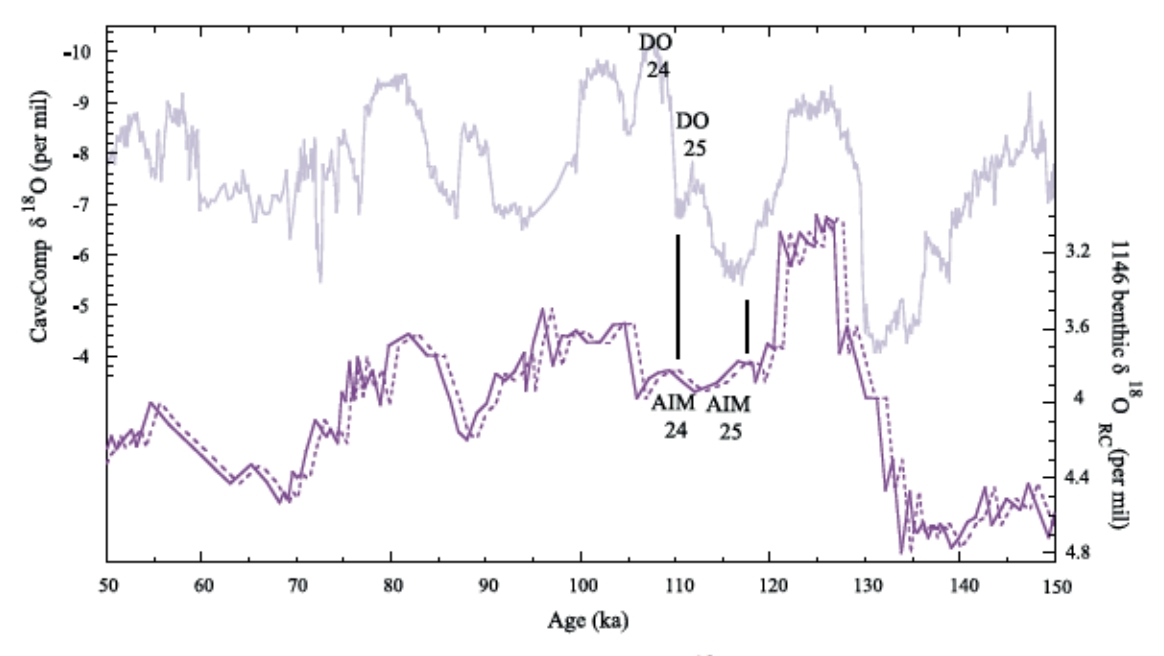


Figure 4. Comparing DO and AIM events. Cave speleothem  $\delta^{18}O$  (top, light purple) and ODP 1146 benthic  $\delta^{18}O$  (bottom, solid and dashed dark purple lines). ODP 1146  $\delta^{18}O$  in solid dark purple line is plotted on the RC chronology (see text). ODP 1146 benthic  $\delta^{18}O$  in dashed dark purple line is plotted on the RC age shifted by 1 kyr, representing a minimum ventilation age offset.

less than 1% the estimated age [Wang et al., 2001, 2008] or under 1000 years.

## 3.3. Age Models

[9] The RC age model was created for ODP 1146 MIS 5 by aligning the ODP 1146 planktic  $\delta^{18}$ O record to the speleothem  $\delta^{18}$ O record using the Lisiecki and Lisiecki [2002]. Match program (R. P. Caballero-Gill et al., Direct correlation of Chinese speleothem  $\delta^{18}$ O and South China Sea planktonic  $\delta^{18}$ O: Transferring a speleothem chronology to the benthic marine chronology, submitted to Paleoceanography, 2011), which uses dynamic programming to align time series. Prior to aligning the two records, the planktic δ18O record was filtered to eliminate the influence of eccentricity because the speleothem record lacks this 100 kyr influence. The MIS 5 portion of the planktic  $\delta^{18}$ O record was aligned to the speleothem  $\delta^{18}$ O using 3 tie points, at 60.02, 109.69, and 129.71 kyr (Figure 3). The resulting age model was transferred directly to the ODP 1146 benthic  $\delta^{18}$ O record, derived from the same samples.

# 4. Results

[10] Using the RC chronology, the 1146 benthic  $\delta^{18}O$  record includes additional structures within MIS 5.4 not previously identified in deep ocean  $\delta^{18}O$  outside the North Atlantic (Figures 3 and 4). The events are defined by 10 data points (of which 7 were replicated at least once), characterized by an isotopic range of 0.16 ‰, and are within a continuous interval (no core breaks). Following traditional nomenclature [Prell et al., 1986] we identify these events as MIS 5.4.2, 5.4.3, 5.4.4, 5.4.5 and 5.4.6 (Figure 3). The duration of isotopic events 5.4.6–5.4.4 is 6.4 kyr, with  $\delta^{18}O$  change of 0.16 ‰; the duration of isotopic events 5.4.4–5.4.2 is 6.1 kyr, with  $\delta^{18}O$  change of 0.15 ‰.

[11] Similar to the CH<sub>4</sub>-synchronized ice core records, events MIS 5.4.3 and MIS 5.4.5 in the 1146 benthic  $\delta^{18}$ O are out of phase and lead DO events 24 and 25 in speleothem  $\delta^{18}$ O [Kelly et al., 2006] (Figure 4). This out of phase relationship indicates that the deep ocean  $\delta^{18}$ O becomes depleted prior to processes driving the surface  $\delta^{18}$ O responses of speleothem calcite and planktic foraminifera toward depleted values. Lead of benthic  $\delta^{18}$ O relative to surface  $\delta^{18}$ O becomes more evident when ventilation rates are taken into account (Figure 4).

## 5. Discussion

[12] Transfer of the speleothem chronology to the 1146 record (the RC chronology) is justified on the basis that both speleothem and Gs. ruber  $\delta^{18}$ O respond to the same set of surface environmental controls at annual to orbital time scales. Using the RC age model, comparison of speleothem  $\delta^{18}$ O [Wang et al., 2008] and ODP 1146 benthic  $\delta^{18}$ O indicates that the older 1146 event (MIS 5.4.5) occurs just prior to DO 25 in the speleothem  $\delta^{18}$ O (Figure 4). Similarly, the younger 1146 benthic  $\delta^{18}$ O event (MIS 5.4.3) occurs prior to DO 24 in the speleothem record. These relationships parallel those in the EDML and NGRIP records when the age models are synchronized using CH4 [Capron et al., 2010]. Thus, we interpret these two benthic  $\delta^{18}$ O events as AIM 24 and 25, documenting the deep ocean response to the bipolar seesaw at a location in the South China Sea, near the end of the deep ocean conveyor belt.

[13] The classical bipolar seesaw concept [Broecker, 1998] relies on the slowing of thermohaline circulation as a trigger for abrupt climate change. As the thermohaline circulation slows, the northern hemisphere cools and the southern hemisphere warms because less heat is transported from the south to the north. This bipolar seesaw concept

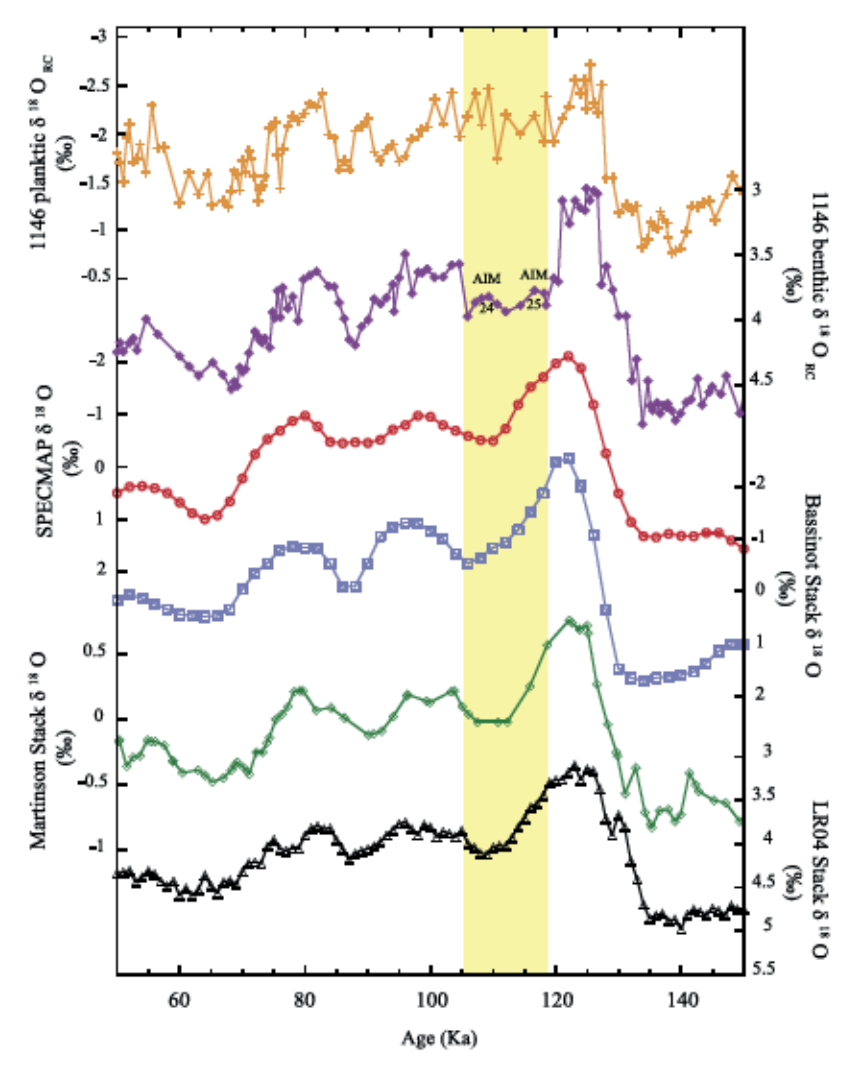


Figure 5. MIS 5 in ODP 1146 and four global stacks. Additional structures found at ODP 1146 benthic  $\delta^{18}O$  (AIM events 24 and 25) are not evident in any of the global stacks. Yellow bar indicates where AIM events fall on ODP 1146 benthic  $\delta^{18}O$  (second record from the top, in purple). References for stacks, from bottom to top: Lisiecki and Raymo [2005], Martinson et al. [1987], Bassinot et al. [1994], and Imbrie et al. [1984]. ODP 1146 data is plotted using the RC age model; all other records plotted using their published chronology.

predicts an out of phase relationship (180°) between the northern and southern hemispheres. The thermal bipolar seesaw is a modification of the classical seesaw, which includes a heat reservoir in the south working on 10<sup>3</sup> timescales [Stocker and Johnsen, 2003].

[14] ODP 1146 sediments are bathed by North Pacific Deep Waters that appear to have varying ventilation ages over time [Sarnthein et al., 2007]. Ventilation ages in the SCS varied from 3.8 kyr near the last glacial maximum to <1.9 kyr during the final stages of the glacial period [Sarnthein et al., 2007], implicating changes in circulation during the last deglaciation as the causal mechanism. Other studies, using cores bathed by Pacific deep waters (depth of 2000 m) north of the equator, use a 1 kyr deep-water transit time, such that benthic  $\delta^{18}$ O lead the surface proxies by 1 kyr [Saikku et al., 2009]. If this 1 kyr ventilation age is applied to ODP 1146, the two light MIS 5.4 warm events would move 1 kyr older, aligning exceptionally well with

heavy (colder) events recorded by speleothem  $\delta^{18}{\rm O}$  from China. This out of phase relationship of  $\delta^{18}{\rm O}$  in speleothem and planktic forams relative to  $\delta^{18}{\rm O}$  in benthic forams supports the thermal bipolar seesaw concept. Using the radiometrically synchronized age scales, the AIM-DO phase relationships expressed in the 1146 and speleothem records are the same as those expressed in the EDML and NGRIP records when placed on CH<sub>4</sub>-synchronized age scales. Direct comparison of 1146 to EDML is not feasible given the error in the ice core chronologies [*Ruth et al.*, 2007]. Compared to the RC age scale, AIM 24 and 25 in the ice core records are  $\sim$ 3.5 and  $\sim$ 5 kyr too young, respectively,

[15] Model simulations of sea level changes during MIS 5.4 [Siddall et al., 2010] bear remarkable similarity to the ODP 1146 benthic  $\delta^{18}$ O suggesting a strong sea level forcing for the benthic  $\delta^{18}$ O AIM events. Phase differences between modeled-sea level and the benthic  $\delta^{18}$ O AIM events could be due to age model differences or to a greater

influence of "Antarctic forcing" on sea level fluctuations [Siddall et al., 2010]. Further evidence of sea level fluctuations during AIM 25 is found in Bahamas corals [Thompson et al., 2011]. Assuming that a 0.011 % shift in  $\delta^{18}$ O equates to 1 m of sea level change [Fairbanks, 1989], the 1146 AIM 24 and 25 events would represent a sea level change of -35 to -38.2 m from present. Comparable sea level changes attributed to millennial scale climate change have been reported for MIS 3 [Siddall et al., 2003]. A contribution from deep-water temperature change to the 1146 AIM 24 and 25 events cannot be ruled out at this point.

[16] Our study documents for the first time the radiometrically calibrated timing of AIM events in deep Pacific  $\delta^{18}$ O during the last interglacial. We have identified published benthic  $\delta^{18}$ O records with enough sampling resolution to show AIM events. These records are located in the North Atlantic [Hodell et al., 2008; Shackleton et al., 2000], Equatorial Atlantic [Castañeda et al., 2009], North Pacific [Herbert et al., 2001], Equatorial Pacific [Shackleton et al., 1983], and South Pacific [Moy et al., 2006; Pahnke and Zahn, 2005]. Regardless of the mechanisms driving isotopic change in deep-ocean waters, identification of AIM events in benthic records from multiple ocean basins indicates that the benthic  $\delta^{18}$ O AIM 24 and 25 events are global in nature and likely reflect changes in terrestrial ice volume.

[17] The global  $\delta^{18}$ O stacks that are used in paleoclimate reconstructions and for chronology do not include millennial-scale structure described above (Figure 5). The main advantage of stacking records is that it minimizes any noise or local effects, resulting in a global signal. Nevertheless, as argued by Shackleton et al. [1990], a significant weakness in the stacking approach is the inclusion of low-resolution records, which serves to average out millennial-scale structure present in high-resolution records; structure that appears global in nature. Another caveat of stacking climate records, as argued by Huybers and Wunsch [2004], is that matching isotopic events assumes such events are globally in phase. One way to resolve the phasing of events is to map such events using absolute dating. Our paper provides one such effort. Including millennial-scale variability in stacked records would also enhance the chronostratigraphic utility of the benthic marine  $\delta^{18}$ O chronology and aid in understanding ocean-atmosphere couplings that are part of the mechanisms driving climate change.

## 6. Conclusions

- [18] A radiometrically calibrated age model for ODP 1146 yields a robust chronology independent of assumptions inherent in orbital tuning. Structures within MIS 5.4, not expressed in global stacked records, are evident in the ODP 1146 benthic  $\delta^{18}$ O record. These isotopic events (5.4.3 and 5.4.5) are anthiphased and lead DO events in southeast Chinese speleothem  $\delta^{18}$ O, consistent with AIM events 24 and 25. We attribute the presence of AIM events in benthic  $\delta^{18}$ O to changes in the isotopic composition of deep waters due to variations in ice volume (sea level), an assertion consistent with the recent model-derived sea level reconstructions.
- [19] Acknowledgments. We thank informal reviewers Timothy D. Herbert and Jan Tullis as well as formal reviewer Mark Siddall; the Editor, Rainer Zahn; and one anonymous reviewer for constructive comment and criticism. This work was supported by U.S. National Science Foundation

grant OCE0352215 to SCC and Graduate STEM K-12 Fellowship to RPCG. Marine samples were provided by the Ocean Drilling Program (ODP). April Martin and Dmitri Sedykin assisted with various aspects of data reduction.

#### References

- Bassinot, F. C., L. Labeyrie, E. Vincent, X. Quidelleur, N. J. Shackleton, and Y. Lancelot (1994), The astronomical theory of climate and the age of the Brunhes-Matuyama magnetic reversal, *Earth Planet. Sci. Lett.*, 126, 91–108, doi:10.1016/0012-821X(94)90244-5.
- Broecker, W. S. (1998), Paleocean circulation during the last deglaciation: A bipolar seesaw?, Paleoceanography, 13, 119–121, doi:10.1029/97PA03707.
- Capron, E., et al. (2010), Synchronising EDML and NorthGRIP ice cores using  $\delta^{18}$ O of atmospheric oxygen ( $\delta^{18}$ O atm) and CH4 measurements over MIS 5(80–123 kyr), *Quat. Sci. Rev.*, 29, 222–234, doi:10.1016/j. quascirev.2009.07.014.
- Castañeda, I. S., S. Mulitza, B. Schefu, E. Lopes dos Santos, R. Simninghe, and J. S. Damsté (2009), Wet phases in the Sahara/Sahel region and human migration patterns in North Africa, *Proc. Natl. Acad. Sci. U. S. A.*, 106, 20,159–20,163.
- Clemens, S. C., W. L. Prell, Y. Sun, Z. Liu, and G. Chen (2008), Southern Hemisphere forcing of Pliocene δ<sup>18</sup>O and the evolution of Indo-Asian monsoons, *Paleoceanography*, 23, PA4210, doi:10.1029/2008PA001638.
  Clemens, S. C., W. L. Prell, and Y. Sun (2010), Orbital-scale timing and
- Clemens, S. C., W. L. Prell, and Y. Sun (2010), Orbital-scale timing and mechanisms driving late Pleistocene Indo-Asian summer monsoons: Reinterpreting cave speleothem δ<sup>18</sup>O, Paleoceanography, 25, PA4207, doi:10.1029/2010PA001926.
- Fairbanks, R. G. (1989), A 17,000-year glacio-eustatic sea level record: Influence of glacial melting rates on the Younger Dryas event and deep-ocean circulation, *Nature*, 342, 637–642, doi:10.1038/342637a0.
- Greenland Ice-Core Project Members (1993), Climate instability during the last interglacial period recorded in the GRIP ice core, *Nature*, 364, 203–207, doi:10.1038/364203a0.
- Greenland Ice-Core Project Members (2004), High-resolution record of Northern Hemisphere climate extending into the last interglacial period, Nature, 431, 147–151, doi:10.1038/nature02805.
- Grootes, P. M., M. Stuiver, J. W. C. White, S. J. Johnsen, and J. Jouzel (1993), Comparison of oxygen isotope records from the GISP2 and GRIP Greenland ice cores, *Nature*, 366, 552–554, doi:10.1038/366552a0.
- Herbert, T. D., J. D. Schuffert, D. Andreasen, L. Heusser, M. Lyle, A. Mix, A. C. Ravelo, L. D. Stott, and J. C. Herguera (2001), Collapse of the California current during glacial maxima linked to climate change on land, *Science*, 293, 71–76, doi:10.1126/science.1059209.
- Hodell, D. A., J. E. T. Channell, J. H. Curtis, O. E. Romero, and U. Röhl (2008), Onset of "Hudson Strait" Heinrich events in the eastern North Atlantic at the end of the middle Pleistocene transition (~640 ka)?, Paleoceanography, 23, PA4218, doi:10.1029/2008PA001591.
- Huybers, P., and C. Wunsch (2004), A depth derived Pleistocene age model: Uncertainty estimates, sedimentation variability, and nonlinear climate change, *Paleoceanography*, 19, PA1028, doi:10.1029/2002PA000857.
- Imbrie, J., J. D. Hays, D. Martinson, A. McIntyre, A. C. Mix, J. J. Morley, N. G. Pisias, W. L. Prell, and N. J. Shackleton (1984), The orbital theory of Pleistocene climate: Support from a revised chronology of the marine δ<sup>18</sup>O record, in *Milankovitch and Climate*, Part 1, edited by A. L. Berger, et al., pp. 269–305, D. Reidel, Hingham, Mass.
- Jiang, D., X. Lang, Z. Tian, and D. Guo (2011), Last Glacial Maximum Climate over China from PMIP simulations, *Palaeogeogr. Palaeocli-matol. Palaeoecol.*, 309, 347–357, doi:10.1016/j.palaeo.2011.07.003.
- Kalnay, E., et al. (1996), The NCEP/NCAR Reanalysis 40-year Project, Bull. Am. Meteorol. Soc., 77, 437–471, doi:10.1175/1520-0477(1996) 077<0437:TNYRP>2.0.CO:2.
- Kelly, M. J., R. L. Edwards, H. Cheng, D. Yuan, Y. Cai, M. Zhang, Y. Lin, and Z. An (2006), High resolution characterization of the Asian Monsoon between 146,000 and 99,000 years B.P. from Dongge Cave, China and global correlation of events surrounding Termination II, Palaeogeogr. Palaeoclimatol. Palaeoecol., 236, 20–38, doi:10.1016/j.palaeo.2005. 11.042.
- Kutzbach, J. E., X. Liu, Z. Liu, and G. Chen (2008), Simulation of the evolutionary response of global summer monsoons to orbital forcing over the past 280,000 years, Clim. Dyn., 30, 567–579, doi:10.1007/s00382-007-0308-z.
- Lisiecki, L. E., and P. A. Lisiecki (2002), Application of dynamic programming to the correlation of paleoclimate records, *Paleoceanography*, 17(4), 1049, doi:10.1029/2001PA000733.
- Lisiecki, L. E., and M. E. Raymo (2005), A Pliocene-Pleistocene stack of 57 globally distributed benthic δ<sup>18</sup>O records, *Paleoceanography*, 20, PA1003, doi:10.1029/2004PA001071.

- Martinson, D. G., N. G. Pisias, J. D. Hays, J. D. Imbrie, T. C. Moore, and N. J. Shackleton (1987), Age Dating and the orbital theory of the ice ages: Development of a high-resolution 0 to 300,000-year chronostratigraphy, *Quat. Res.*, 27, 1–29, doi:10.1016/0033-5894(87)90046-9.
  Martrat, B., J. O. Grimalt, N. J. Shackleton, L. Abreu, M. A. Hutterli,
- Martrat, B., J. O. Grimalt, N. J. Shackleton, L. Abreu, M. A. Hutterli, and T. F. Stocker (2007), Four climate cycles of recurring deep and surface water destabilizations on the Iberian Margin, *Science*, 317, 502–507, doi:10.1126/science.1139994.
- Moy, A. D., W. R. Howard, and M. K. Gagan (2006), Late Quaternary palaeoceanography of the Circumpolar Deep Water from the South Tasman Rise, J. Quat. Sci., 21, 763–777, doi:10.1002/jqs.1067.
- Pahnke, K., and R. Zahn (2005), Southern Hemisphere water mass conversion linked with North Atlantic climate variability, Science, 307, 1741–1746, doi:10.1126/science.1102163.
- Prell, W. L., J. Imbrie, D. G. Martinson, J. J. Morley, N. G. Pisias, N. J. Shackleton, and H. F. Streeter (1986), Graphic correlation of oxygen isotope stratigraphy application to the late Quaternary, *Paleoceanography*, 1, 137–162, doi:10.1029/PA001i002p00137.
- Ruth, U., et al. (2007), EDML1: A chronology for the EPICA deep ice core from Dronning Maud Land, Antarctica, over the last 150 000 years, Clim. Past, 3, 475–484, doi:10.5194/cp-3-475-2007.
- Saikki, R., L. Stott, and R. Thunell (2009), A bi-polar signal recorded in the western tropical Pacific: Northern and Southern Hemisphere climate records from the Pacific warm pool during the last Ice Age, Quat. Sci. Rev., 28, 2374–2385, doi:10.1016/j.quascirev.2009.05.007.
- Sarnthein, M., P. M. Grootes, J. P. Kennett, and M.-J. Nadeau (2007), 14C reservoir ages show deglacial changes in ocean currents and carbon cycle, in Ocean Circulation: Mechanisms and Impacts—Past and Future Changes of Meridional Overturning, Geophys. Monogr. Ser, vol. 173, edited by A. Schmittner, J. C. H. Chiang, and S. R. Hemming, pp. 175–196, AGU, Washington, D. C., doi:10.1029/173GM13
- Shackleton, N. J., M. A. Hall, J. Line, and C. Shuxi (1983), Carbon isotope data in core V19–30 confirm reduced carvon dioxide concentration in the ace age atmosphere, *Nature*, 306, 319–322, doi:10.1038/306319a0.
- Shackleton, N. J., A. Berger, and W. R. Peltier (1990), An alternative astronomical calibration of the Lower Pleistocene timescale based on ODP Site 677, Trans. R. Soc. Edinburgh Earth Sci., 81, 251–261, doi:10.1017/S0263593300020782.
- Shackleton, N. J., M. A. Hall, and E. Vincent (2000), Phase relationships between millennial-scale events 64,000–24,000 years ago, *Paleoceano-graphy*, 15, 565–569, doi:10.1029/2000PA000513.
- Siddall, M., E. J. Rohling, A. Almogi-Labin, C. Hemleben, D. Meischner, I. Schmelzer, and D. A. Smeed (2003), Sea-level fluctuations during the last glacial cycle, *Nature*, 423, 853–858, doi:10.1038/nature01690.

- Siddall, M., M. R. Kaplan, J. M. Schaefer, A. Putnam, M. Kelly, and B. Goehring (2010), Changing influence of Antarctic and Greenlandic temperature records on sea-level over the last glacial cycle, *Quat. Sci. Rev.*, 29, 410–423, doi:10.1016/j.quascirev.2009.11.007.
- Steinke, S., M. Kienast, J. Groeneveld, L.-C. Lin, M.-T. Chen, and R. Rendle-Bühring (2008), Proxy dependence of the temporal pattern of deglacial warming in the tropical South China Sea: Toward resolving seasonality, Quat. Sci. Rev., 27, 688–700, doi:10.1016/j.quascirev.2007. 12.003.
- Stocker, T. F., and S. J. Johnsen (2003), A minimum thermodynamic model for the bipolar seesaw, *Paleoceanography*, 18(4), 1087, doi:10.1029/ 2003PA000920.
- Thompson, W. G., H. A. Curran, M. A. Wilson, and B. White (2011), Sealevel oscillations during the last interglacial highstand recorded by Bahamas corals, *Nat. Geosci.*, 4, 684–687, doi:10.1038/ngco1253.
- Tian, J., P. Wang, R. Chen, and X. Cheng (2005), Quaternary upper ocean thermal gradient variations in the South China Sea: Implications for east Asian monsoon climate, *Paleoceanography*, 20, PA4007, doi:10.1029/ 2004PA001115.
- Voelker, A. H. L. (2002), Global distribution of centennial-scale records for Marine Isotope Stage (MIS) 3: A database, Quat. Sci. Rev., 21, 1185–1212, doi:10.1016/S0277-3791(01)00139-1.
- Wang, Y. J., H. Cheng, R. L. Edwards, Z. S. An, J. Y. Wu, C. C. Shen, and J. A. Dorale (2001), A high-resolution absolute-dated late Pleistocene monsoon record from Hulu Cave, China, Science, 294, 2345–2348, doi:10.1126/science.1064618.
- Wang, Y. J., H. Cheng, R. L. Edwards, Y. He, X. Kong, Z. An, J. Wu, M. J. Kelly, C. A. Dykoski, and X. Li (2005), The Holocene Asian monsoon: Links to solar changes and North Atlantic climate, *Science*, 308, 854–857, doi:10.1126/science.1106296.
- Wang, Y., J. H. Cheng, R. L. Edwards, X. G. Kong, X. H. Shao, S. T. Chen, J. Y. Wu, X. Y. Jiang, X. F. Wang, and Z. S. An (2008), Millennialand orbital-scale changes in the East Asian monsoon over the past 224,000 years, *Nature*, 451, 1090–1093, doi:10.1038/nature06692.
- Wiesner, M. G., L. F. Zheng, and H. K. Wong (1996), Fluxes of particulate matter in the South China Sea, in *Particle Flux in the Ocean*, edited by V. Ittekkot et al., pp. 91–154, John Wiley, Hoboken, N. J.

R. P. Caballero-Gill, S. Clemens, and W. Prell, Department of Geological Sciences, Brown University, 324 Brook St., Providence, RI 02912, USA. (rocio caballero@brown.edu)